

Geophysical Research Letters

RESEARCH LETTER

10.1029/2020GL088918

Key Points:

- Hillslope aspect controls vegetation greenness in semiarid ecosystems
- Polar-facing slopes do not always have higher NDVI than equatorial-facing slopes
- The change in NDVI patterns is attributed to vegetation phenology and climate seasonality

Supporting Information:

- Supporting Information S1

Correspondence to:

O. Yetemen,
yetemen@itu.edu.tr

Citation:








Kumari, N., Saco, P. M., Rodriguez, J. F., Johnstone, S. A., Srivastava, A., & Chun, K. P., et al. (2020). The grass is not always greener on the other side: Seasonal reversal of vegetation greenness in aspect-driven semiarid ecosystems. *Geophysical Research Letters*, 47, e2020GL088918. <https://doi.org/10.1029/2020GL088918>

Received 27 MAY 2020

Accepted 3 JUL 2020

Accepted article online 8 JUL 2020

The Grass Is Not Always Greener on the Other Side: Seasonal Reversal of Vegetation Greenness in Aspect-Driven Semiarid Ecosystems

Nikul Kumari¹ , Patricia M. Saco¹ , Jose F. Rodriguez¹ , Samuel A. Johnstone² , Ankur Srivastava¹ , Kwok P. Chun³ , and Omer Yetemen^{1,4} 

¹Discipline of Civil, Surveying and Environmental Engineering, The University of Newcastle, Callaghan, New South Wales, Australia, ²U.S. Geological Survey, Geosciences and Environmental Change Science Center, Denver, CO, USA, ³Department of Geography, Hong Kong Baptist University, Hong Kong, China, ⁴Eurasia Institute of Earth Sciences, Istanbul Technical University, Istanbul, Turkey

Abstract Our current understanding of semiarid ecosystems is that they tend to display higher vegetation greenness on polar-facing slopes (PFS) than on equatorial-facing slopes (EFS). However, recent studies have argued that higher vegetation greenness can occur on EFS during part of the year. To assess whether this seasonal reversal of aspect-driven vegetation is a common occurrence, we conducted a global-scale analysis of vegetation greenness on a monthly time scale over an 18-year period (2000–2017). We examined the influence of climate seasonality on the normalized difference vegetation index (NDVI) values of PFS and EFS at 60 different catchments with aspect-controlled vegetation located across all continents except Antarctica. Our results show that an overwhelming majority of sites (70%) display seasonal reversal, associated with transitions from water-limited to energy-limited conditions during wet winters. These findings highlight the need to consider seasonal variations of aspect-driven vegetation patterns in ecohydrology, geomorphology, and Earth system models.

Plain Language Summary Sunny (equatorial-facing) slopes receive more solar radiation than shady (polar-facing) slopes. A common assumption in water-limited semiarid ecosystems is that this difference in solar radiation results in shady slopes being greener than sunny slopes, because they lose less water to the atmosphere due to evapotranspiration. Some studies have suggested seasonal changes to this pattern, but the lack of a global-scale analysis has prevented a clear understanding of the extent of this phenomenon and its causes. Here, we used an 18-year record of remotely sensed monthly data to compare vegetation activity on opposing slopes in 60 semiarid catchments with different climates from all over the world. Our results show three different patterns: (1) always greener shady slopes; (2) greener shady slopes in summer but greener sunny slopes in winter; and (3) no discernible difference between slopes. Contrary to the common belief that shady slopes are always greener in semiarid landscapes, the majority of the studied sites show a seasonal reversal of this patterns in vegetation greenness. We attribute this contrasting behavior to the timing of precipitation and different growth responses of vegetation types on opposing slopes. At sites having wet winters, sunny slopes benefit more from solar radiation; hence, their vegetation grows more rapidly than that of shady slopes. These findings underline the importance of considering the seasonal variations of vegetation pattern on opposing slopes in ecohydrological, geomorphological, and Earth system models.

1. Introduction

Variations in insolation between opposing polar-facing slopes (PFS) and equatorial-facing slopes (EFS) can be up to ~30% for moderate hillslope gradients at midlatitudes (Del-Toro-Guerrero et al., 2019; Zou et al., 2007). These differences generate contrasting micrometeorological conditions, mainly in air temperature and potential evapotranspiration (PET), which drives differences in available soil moisture (Branson & Shown, 1989; Metzen et al., 2019). These microclimatic variations result in a relatively cooler and mesic environment on PFS and a relatively warmer and xeric environment on EFS. Hence, aspect-driven

©2020. The Authors.

This is an open access article under the terms of the Creative Commons Attribution License, which permits use, distribution and reproduction in any medium, provided the original work is properly cited.

ecosystems, characterized by differences in vegetation density and type, emerge as a result of variations in insolation (e.g., Flores-Cervantes et al., 2014; Pelletier & Swetnam, 2017; Sternberg & Shoshany, 2001). These distinct variations for opposing hillslope aspects are more pronounced in semiarid ecosystems as they tend to exhibit strong feedbacks between soil moisture and vegetation.

Studies from the ecology, soil science, hydrology, and geomorphology communities have been conducted at different locations throughout the world to understand the implications of aspect-controlled ecosystems on vegetation type, density, biodiversity, and phenology (Broza et al., 2004; Caylor et al., 2004; Kirkpatrick & Nunez, 1980; Nobel & Linton, 1997); chemical composition of soils (Klemmedson & Wienhold, 1992; Román-Sánchez et al., 2018) and plants (Vetaas, 1992; Xu et al., 2017); soil moisture (Cantón et al., 2004; Geroy et al., 2011); runoff production, erosion, and resulting landscape form (Hinckley et al., 2014; Yetemen et al., 2015; Richardson et al., 2020); and wildfire risks (Calviño-Cancela et al., 2017; Walsh et al., 2017). These studies report that denser and mesic vegetation is usually dominant on PFS, while EFS are occupied by sparser and xeric plants in both the Northern Hemisphere (NH) (Nevo, 1995; Sternberg & Shoshany, 2001) and the Southern Hemisphere (SH) (Armesto & Martinez, 1978; Badano et al., 2005).

Much of the previous research on aspect-controlled ecosystems is based on field observations, which provide important details but are obtained over short time periods (mostly the growing season). In addition, results from these studies are based on a limited number of field plots on opposing hillslope aspects, which leads to lack of uniformity and homogeneity in the monitoring process (Barbosa et al., 2006; Lawley et al., 2016). These limitations can be partially addressed by using remote-sensed vegetation indices (VIs), as they provide temporally regular and spatially distributed data with consistent coverage for the assessment of vegetation dynamics (Becerril-Piña et al., 2015; Hoek van Dijke et al., 2019; Lawley et al., 2016; Wallace et al., 2006). VIs combine two or more spectral bands, and their use for assessing ecological properties of vegetation has dramatically increased over the last two decades (Asner & Martin, 2009; Moreno-De Las Heras et al., 2012; Nagendra, 2001). The normalized difference vegetation index (NDVI), which compares the intensity of reflectance in the visible red and near-infrared bands, is the most commonly used VI to quantify the presence of live green vegetation (Rouse et al., 1973). By relying on a ratio of band intensities, NDVI removes a large proportion of noise caused by cloud shadows, topographic and solar angle variations, and atmospheric attenuations existing in visible red and infrared bands, which makes NDVI less susceptible to illumination conditions (Huete et al., 2002; Justice et al., 1981; Martín-Ortega et al., 2020). NDVI values have been used as a proxy for vegetation greenness in hillslope-scale studies looking at differences in vegetation between hillslope aspects (e.g., Del Toro-Guerrero et al., 2016; Jin et al., 2009). These studies found that, in those particular catchments, PFS have higher values of NDVI than their corresponding EFS throughout the year due to differences in solar radiation.

Recent research, however, challenges the general understanding that vegetation greenness is higher on PFS than on EFS, particularly for areas in which transitions between water-limited and energy-limited conditions for plant growth occur (Fan et al., 2019; Johnstone et al., 2017; Yetemen et al., 2015). Modeling results for aspect-controlled semiarid ecosystems in monsoonal semiarid climates (Yetemen et al., 2015) suggest that EFS can briefly display higher vegetation greenness than PFS during the growing season because they benefit more from summer rainfall; however, this advantage may not last long due to the fast depletion of available water. In individual catchments in Gabilan Mesa, California, USA, Johnstone et al. (2017) also found higher values of NDVI on EFS during winter, coinciding with the rainy season, and a return to higher NDVI on PFS during summer.

The complex relations between water, energy, and vegetation across PFS and EFS constitute some of the lesser understood issues in global change research and Earth systems modeling (Fan et al., 2019). Although there is some evidence that transitions between water-limited and energy-limited phases of semiarid ecosystems may challenge the current paradigm of higher vegetation greenness on PFS, there has been no global study to verify this assertion. Here, we present vegetation, topographic, and climatic data from 60 catchments located across all continents, except Antarctica, that allow us to analyze global patterns of vegetation in aspect-controlled ecosystems. We investigate if reversals of higher vegetation greenness patterns from PFS to EFS are common features of aspect-controlled semiarid ecosystems and the conditions under which such reversals occur.

2. Data and Methods

2.1. Study Sites

A careful review of previous studies reporting the existence of pronounced aspect-induced differences in vegetation was undertaken in order to select study sites with minimal anthropogenic impacts. In addition, each site was also visually inspected using Google Earth™ to further assess the lack of anthropogenic activities so that they can be assumed to be in near pristine conditions.

In order to minimize topographic-illumination bias in NDVI, we did not include sites with rugged topographies or at high latitude locations (Holben & Justice, 1980; Moreira & Valeriano, 2014; Teillet et al., 1982). While varying illumination conditions caused by topography have been observed to have negligible impacts on NDVI applications due to its band-ratio format (Matsushita et al., 2007), they still can produce some bias especially on rugged, steep terrain with low solar angles. We only included sites with mean catchment steepness lower than $\sim 25^\circ$ and located at latitudes lower than 45° . We also verified that the topographic-illumination effect was negligible at our selected sites (Figure S1 in the supporting information).

Based on these considerations, a total of 60 different catchments across 23 sites worldwide were selected for this study (Figure 1). Most of these study sites are located in water-limited ecosystems at midlatitudes. Around 52% of these sites are situated in the United States, within the states of Arizona, California, Colorado, and New Mexico. Sites outside the United States were selected in Australia, Chile, Spain, and Sudan (Table S1). According to the descriptions given in previous studies (Table S1), vegetation at these sites is characterized by mesic and relatively dense ground cover on the PFS and xeric and sparse vegetation on the EFS.

The size of the study catchments ranges from ~ 0.5 to 200 km^2 . The mean elevations and slopes of these sites vary from 300 to 2,600 m and $\sim 5^\circ$ to 25° , respectively. These regions have a variety of semiarid climate conditions, including monsoon-influenced continental and Mediterranean climates. Mean annual temperatures range from 5°C to 24°C , and mean annual precipitation (MAP) ranges from 130 to 760 mm. Descriptions of the site locations and the corresponding references to the published studies are given in Table S1.

2.2. Climatic and Topographic Data Sets

Climate data for this study include monthly mean values of temperature and total precipitation at $\sim 1 \text{ km}^2$ spatial resolution (Fick & Hijmans, 2017) obtained from WorldClim2 (<http://worldclim.org>). Corresponding PET values calculated using data from WorldClim2 were obtained from CGIAR-CSI (Zomer et al., 2008). NDVI data derived from Landsat 5, 7, and 8 were downloaded from Google Earth Engine (GEE)™ (Gorelick et al., 2017) for the last 18 years (2000–2017). For this same period, we also downloaded Landsat 7 normalized difference snow index (NDSI) (Dozier, 1989; Rittger et al., 2013) composite data from GEE. The 32-day composites of Landsat data for both NDVI and NDSI are available at the 30-m spatial resolution. The topographic analysis of all catchments was performed using 30-m resolution digital elevation models (DEMs) obtained from GEE (<https://www2.jpl.nasa.gov/srtm/>) (Farr et al., 2007). We chose this spatial resolution of the DEMs because it was the highest available for all catchments; however, we also carried out computations with 10-m resolution DEMs on selected catchments for comparison (Figures S2 and S3). The chosen data sets provide enough spatial resolution to compare vegetation at the hillslope scale, and they are publicly available.

2.3. Methods

The combined information from NDVI and catchment topography was used to identify the spatio-temporal variations of vegetation on different hillslope aspects. Slope, aspect, and elevation for each catchment were first determined from the DEM data. A sink-filling algorithm in ArcGIS (ESRI, 2015) was used to fill the internal depressions and enable the identification of a continuous drainage network for accurate catchment delineation. Hillslope aspect data were segregated into four cardinal directions measured clockwise ($N = 315\text{--}360^\circ$ and $0\text{--}45^\circ$; $E = 45\text{--}135^\circ$; $S = 135\text{--}225^\circ$; $W = 225\text{--}315^\circ$). The north (south) aspects were considered as PFS in the NH (SH) and the south (north) aspects as EFS in the SH (NH).

The spatio-temporal variation of NDVI on different aspects can reveal differences in vegetation phenology and cover (Del Toro-Guerrero et al., 2016). In semiarid ecosystems, which are generally characterized by low to moderate values of NDVI (rarely reaching saturation levels), the dependence of NDVI value on

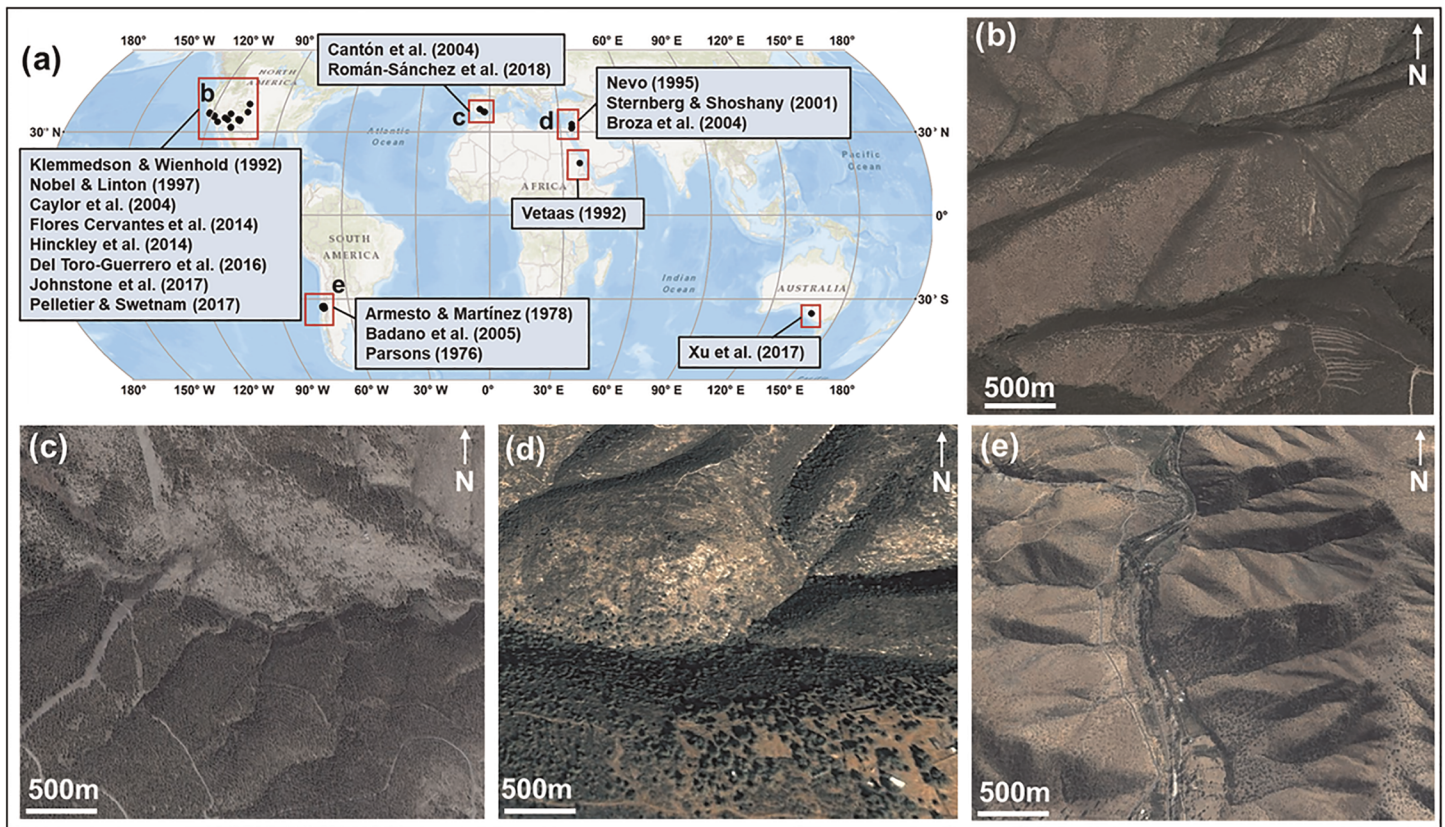


Figure 1. (a) Location of study sites used in this research based on previous work reporting aspect-controlled vegetation patterns; images taken from Google Earth™ at (b) Gabilan Mesa, California, USA; (c) Tabernas Desert, Spain; (d) Nahal Oren, Israel; and (e) Robles Hills, Chile.

vegetation phenology and cover is strong and linear (Fensholt et al., 2004; Huete et al., 2002). Hence, NDVI was used as a surrogate for vegetation greenness on opposing hillslopes in our analysis. NDVI values range between -1 and 1 , but we ignored the negative values because they correspond to lack of vegetation (Pettorelli et al., 2005).

Locations that receive snow cover may generate uncertainty in the values of NDVI, as snow cover increases NDVI values in the same way as vegetation growth (Shabanov et al., 2002). To identify the potential interference of snow in our NDVI analysis, we used NDSI, a commonly used metric to detect and estimate snow cover. NDSI is defined as the ratio of the difference between visible green and shortwave near-infrared bands to the sum of these two bands. NDSI values range from -1 to 1 , with higher values of NDSI representing greater snow cover. In this study, two different NDSI thresholds are considered for detecting snow presence: 0 and 0.1 . These thresholds (0 and 0.1) represent a conservative approach and are substantially lower than the widely used threshold of 0.4 (Klein et al., 1998; Riggs et al., 2017).

For every catchment, we calculated the monthly mean NDVI and NDSI values for the study period (2000–2017) on PFS and EFS separately, based on the aspect data obtained from the topographic analysis. To quantify the relative contrast in NDVI with aspect, we calculated the difference between monthly mean values of NDVI on PFS and EFS, $NDVI_{diff}$, (Johnstone et al., 2017),

$$NDVI_{diff} = NDVI_{PFS} - NDVI_{EFS} \quad (1)$$

where $NDVI_{PFS}$ and $NDVI_{EFS}$ refer to the monthly mean NDVI values within a catchment measured on PFS and EFS, respectively. To quantify the significance of the results, we tested the hypothesis that monthly mean values of NDVI on PFS and EFS are statistically different in all catchments by using the Student's t test. Finally, we analyzed the seasonal variations of $NDVI_{diff}$ across the PFS and EFS in relation to NDSI, precipitation, and PET.

3. Results

Seasonal variations of $NDVI_{diff}$ for all catchments can be classified into three distinct patterns: (a) Type I pattern: $NDVI_{diff}$ is positive throughout the year; (b) Type II pattern: $NDVI_{diff}$ is positive during the summer, but a seasonal reversal leads to a negative value during the winter; and (c) Type III pattern: $NDVI_{diff}$ is very low or negligible for a large part or the entire year. All three $NDVI_{diff}$ patterns are observed at different sites in the NH; however, sites in the SH exhibit only a Type II pattern.

Figure 2 displays the values of $NDVI_{diff}$, which are significant according to Student's t test at $\alpha = 0.05$ ($p < 0.001$), for all the study catchments over the study period. Blue colors represent positive values of $NDVI_{diff}$, indicating that the PFS has greater NDVI than the EFS. Similarly, red colors represent negative values of $NDVI_{diff}$ when NDVI is higher for EFS than for PFS. $NDVI_{diff}$ values between -0.01 and 0.01 are considered negligible (white color). The figure shows that a number of sites in the NH display a Type I $NDVI_{diff}$ pattern, where PFS has greater NDVI than the EFS. This is indeed the case for the catchments at Gordon Gulch (40°N), Colorado; at Kendall (31°N) and two of the sites in Hualapai (35°N), Arizona; and at Guadalupe (32°N), Mexico.

The Type II $NDVI_{diff}$ pattern, showing a seasonal reversal in $NDVI_{diff}$, is the most frequent pattern ($\sim 70\%$ of all the sites) observed among the studied catchments. Catchments at Gabilan Mesa (37°N) and Lower Kern (35°N) in California and East Kaibab (37°N) and Battle Flat ($\sim 34^{\circ}\text{N}$) in Arizona show this seasonal reversal in $NDVI_{diff}$, with positive $NDVI_{diff}$ values in summer and negative $NDVI_{diff}$ (less than -0.01) in winter. Catchments at East Kaibab and Battle Flat in Arizona, where $NDVI_{diff}$ values are negative from November to February, show higher NDVI on PFS than EFS during summer. The Gabilan Mesa and Lower Kern sites from California also show similar reversal behavior, such that $NDVI_{diff}$ in summer is above 0.15 and 0.05 , respectively, while $NDVI_{diff}$ in winter is less than -0.05 .

The Type III $NDVI_{diff}$ pattern is observed mainly at sites in Ramat Avisur, Nahal Oren, and Goral Hills in Israel, at Lucky Hills in Arizona, and a few catchments at Upper Rio Salado in New Mexico. For instance, one of the catchments at Nahal Oren (33°N) shows slightly greater NDVI on PFS than EFS during spring and summer (March–September), with $NDVI_{diff} \sim 0.05$ and the negligible difference between the opposing aspects in other months ($-0.01 < NDVI_{diff} < 0.01$). Catchments at Lucky Hills, Arizona, show a similar pattern with ~ 5 months (June–October) displaying small positive values of $NDVI_{diff}$ but negligible values in other months.

Sites in the SH display only the Type II $NDVI_{diff}$ pattern, possibly because of the relatively limited number of catchments analyzed. Catchments in Chile and Australia show winter reversals in the NDVI pattern. Aconcagua Hills, Robles Hills (33°S), and Corral Quemado (33°S) in Chile show higher NDVI on EFS during austral late spring and summer (October to March) with $NDVI_{diff}$ ranging from 0.02 to 0.2 and $NDVI_{diff}$ decreasing to -0.2 in the austral winter. The Mount Wilson site (35°S) in Australia shows similar NDVI on EFS and PFS during summer. However, in October and November, NDVI on EFS is comparatively higher than PFS ($NDVI_{diff} \sim 0.01$), and winter season shows NDVI reversal.

To account for the potential interference of snow presence in the NDVI analysis (Liu et al., 2013; Shabanov et al., 2002), NDSI values were checked at all catchments. Snow presence at every catchment for each month is reported in Figure 2. The northernmost site in the NH has the largest NDSI values, followed by sites located at high elevations. Also, catchments at East Kaibab, Arizona, located at high elevations ($\sim 2,250$ m above msl) have a considerable snow cover (NDSI > 0.1) from November to February (Billingsley et al., 2008). Similarly, in the SH, Mount Wilson in Australia and Chilean catchments present snow coverage in the austral winter.

As seen in Figure 2, snow-free catchments still display the three observed patterns, especially the Type II $NDVI_{diff}$ pattern. The monthly mean precipitation and PET of all the sites are displayed in Figures S4 and S5, which shows that all sites from California in the NH and Chile in the SH have wet winters and dry summers. The Gabilan Mesa and Lower Kern sites in the NH receive 60–70% of its annual rainfall in the winter months, as do the Chilean sites in the SH. Rainfall in the winter months in the Mediterranean climate favors vegetation growth on the EFS as compared to the PFS.

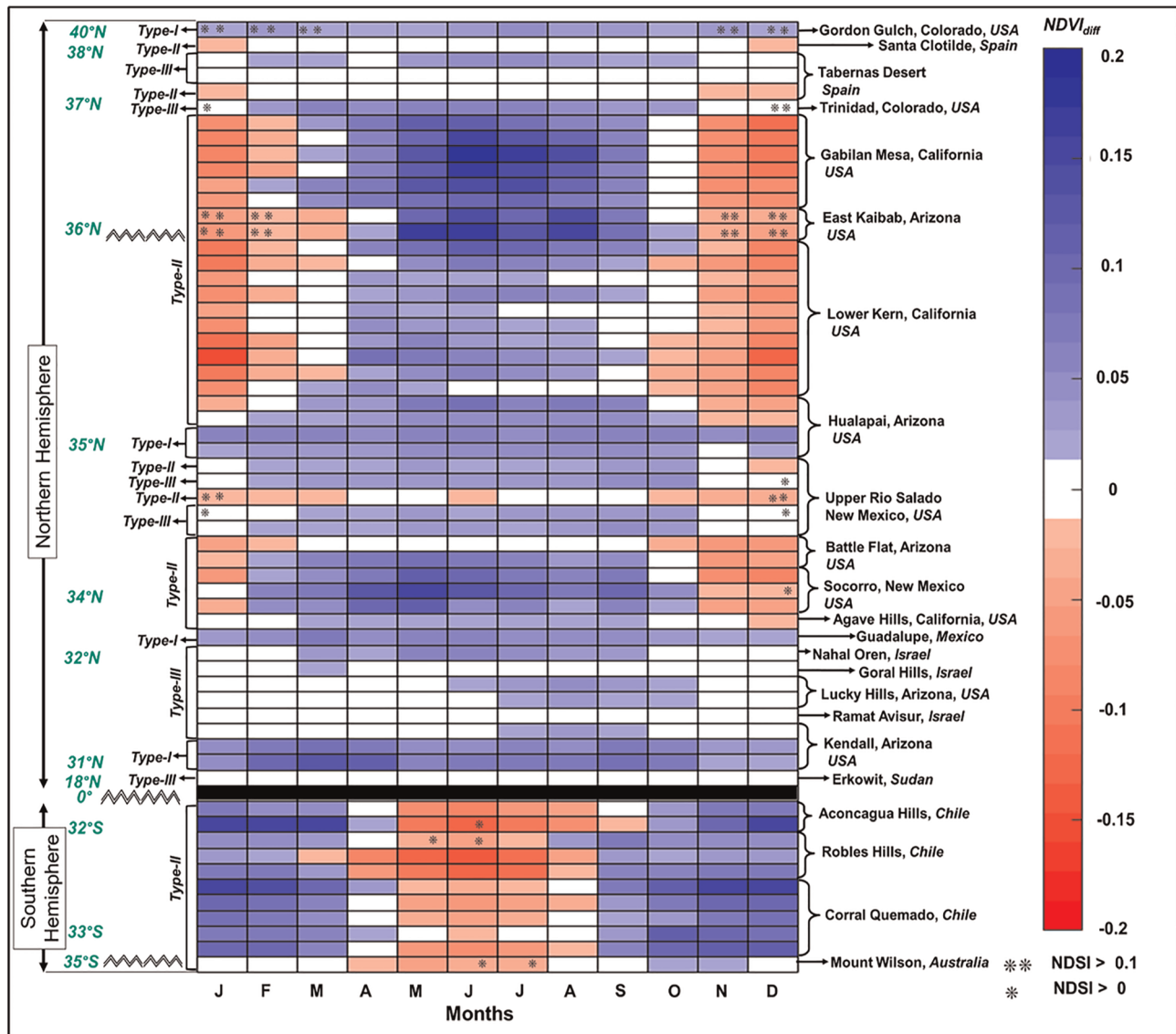


Figure 2. Monthly mean $NDVI_{diff}$ for the period 2000–2017 for all catchments. Snow presence is indicated by (*) when $NDSI > 0.0$ and (**) when $NDSI > 0.1$. Blue and red colors represent positive and negative values of $NDVI_{diff}$, respectively, while negligible $NDVI_{diff}$ is represented by white color.

In order to illustrate and further analyze the different $NDVI_{diff}$ patterns, we show in Figure 3 the three seasonal variation patterns of NDVI with three example sites: Kendall, Arizona (Type I), Gabilan Mesa, California (Type II), and Ramat Avisur, Israel (Type III). Figures 3a and 3d show a Type I $NDVI_{diff}$ pattern, in which NDVI values on PFS are higher than those at EFS and $NDVI_{diff}$ is positive throughout the year. Figures 3b and 3e display the Type II $NDVI_{diff}$ pattern with higher NDVI on PFS in summer and a reversal to negative $NDVI_{diff}$ in winter. Figures 3c and 3f exemplify the Type III $NDVI_{diff}$ pattern observed at Ramat Avisur, Israel, with small values of NDVI and $NDVI_{diff}$ throughout the year.

Figures 3g–3i highlight how monthly PET values at three representative sites follow expected trends in solar insolation. However, seasonal differences in precipitation can produce a switch from water-limited (i.e., $P < PET$) to energy-limited conditions (i.e., $P > PET$). The Kendall site has wet summers under the influence of the North American monsoon (NAM), with monthly PET values always exceeding the corresponding monthly precipitation (Figure 3g). In contrast, Gabilan Mesa has a semiarid Mediterranean climate and monthly precipitation can substantially exceed monthly PET during winter (Figure 3h). Ramat Avisur

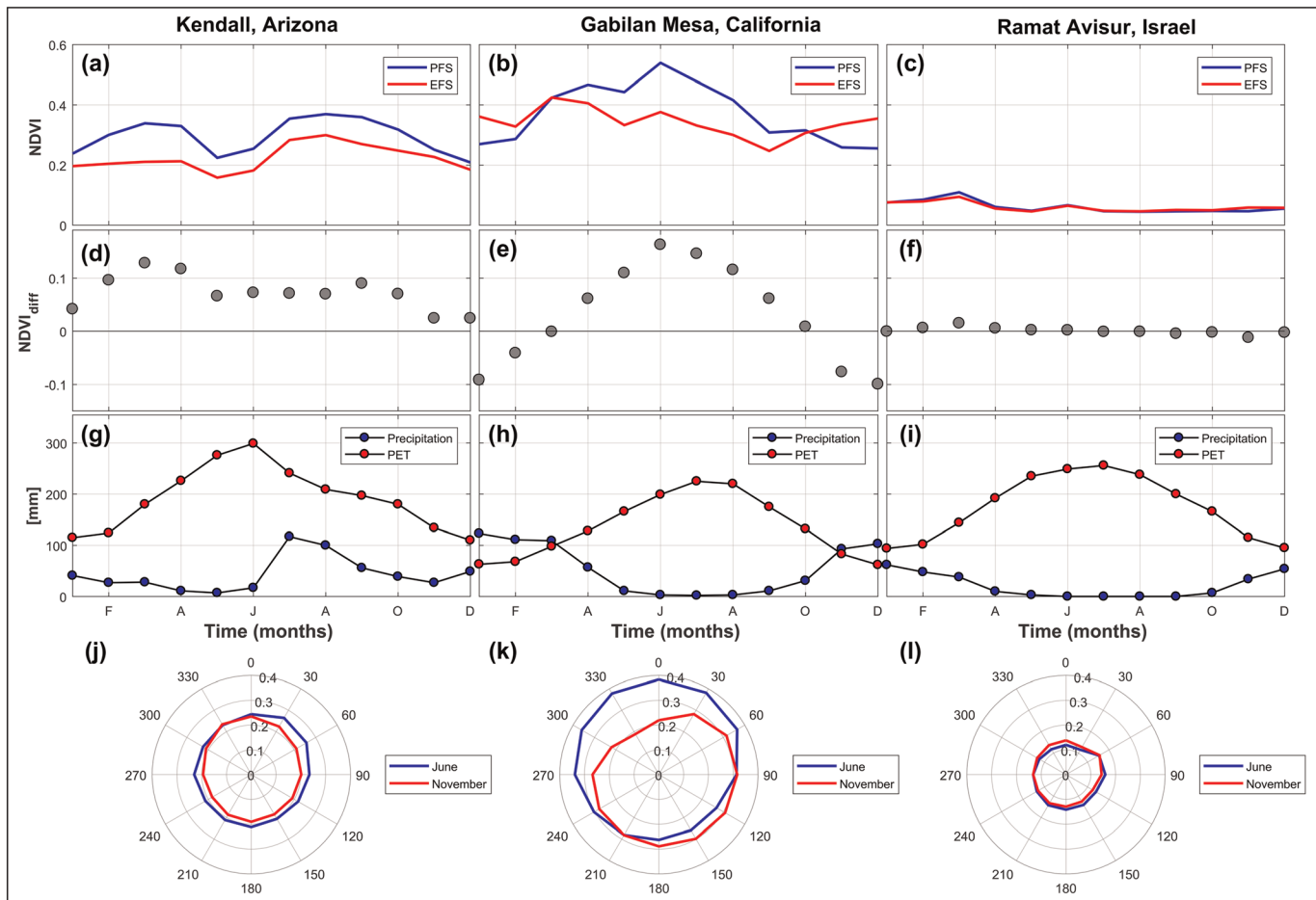


Figure 3. Monthly mean values of NDVI for PFS and EFS aspects (a–c); $NDVI_{diff}$ values (d–f); precipitation (blue circles) and potential evapotranspiration (red circles) (g–j); and binned mean NDVI values for different aspects at 30° intervals for June and November (j–l) for three different patterns: Kendall, Arizona (Type I); Gabilan Mesa, California (Type II); and Ramat Avisur, Israel (Type III).

also has relatively wet winters, although much drier than those at Gabilan Mesa, and monthly PET largely exceeds monthly precipitation (Figure 3i).

To further analyze vegetation variability with respect to all possible aspects, the mean monthly NDVI values were computed at 30° intervals for two selected months, one for NH summer (June) and one for NH winter (November) (Figures 3j–3l). The Kendall site shows that NDVI on PFS (north) is always higher than NDVI on EFS (south) for both June and November (Figure 3j). The seasonal reversals of NDVI at Gabilan Mesa sites show asymmetric response in NDVI values; while higher NDVI values are observed on the northerly aspects (0–60° and 300–360°) in June, the southerly aspects (120–210°) exhibit higher values in November (Figure 3k). NDVI values are similar in both months for the Ramat Avisur site (Figure 3l).

4. Discussion

We found that the Type I $NDVI_{diff}$ pattern, with higher NDVI values on PFS than on EFS throughout the year, occurs only on a small fraction (~8%) of the studied catchments. This pattern agrees with previous field-based observations of a denser canopy on PFS and a sparser cover on EFS (e.g., Armesto & Martinez, 1978; Gutiérrez-Jurado et al., 2006; Sternberg & Shoshany, 2001). This pattern may be attributed to relatively lower insolation and less PET demand on PFS, which reduces the risk of hydraulic failure in plant vascular tissue and plant mortality (Earles et al., 2018; Fan et al., 2019). Surprisingly, the Type I $NDVI_{diff}$ pattern, which would be consistent with the current understanding, is not the dominant pattern in our analysis. However, it is important to note that most previous studies have analyzed data for

particular times of the year (usually the growing season, but see also Del Toro-Guerrero et al., 2016) using both field data (Armesto & Martinez, 1978; Sternberg & Shoshany, 2001) and NDVI (Flores-Cervantes et al., 2014; Kunkel et al., 2011; McGuire et al., 2014).

Our results show that many catchments in both the NH and the SH exhibit a seasonal reversal in $NDVI_{diff}$ (Type II $NDVI_{diff}$ pattern) (Figure 2). Some of the plausible explanations for these reversals in $NDVI_{diff}$ are the potential effect of snow on NDVI values, elevation, climate seasonality, and plant phenology. There are many sites that still show $NDVI_{diff}$ reversal even after excluding snow-affected sites with low/moderate NDSI values. This finding implies that, even though snow interference can affect NDVI observations (Liu et al., 2013), it does not explain the observed seasonal reversal of NDVI for many catchments. Sites located at high elevations (Socorro, Upper Rio Salado, East Kaibab, and Colorado) have low temperatures that may act as a major limiting factor for plant growth. Hence, EFS can benefit from more insolation and have longer growing seasons than PFS leading to early growth on EFS in winter but not sustainable growth in summer (e.g., Salzer et al., 2014; Zhang et al., 2015). Temperature limitation can be a reasonable explanation for $NDVI_{diff}$ reversal for places where severe environmental conditions prevail; however, the elevation of most of the study sites is less than 2,000 m and not prone to extremely cold conditions (Boisvenue & Running, 2006).

Though water availability is the main controlling factor on evapotranspiration in most semiarid ecosystems, some areas may also experience periods of energy limitation during the year as a result of rainfall seasonality (Garcia et al., 2014; Ivanov et al., 2008; Moran et al., 2009). This transition from water limitation to energy limitation is more pronounced when evaporative demand is exceeded by rainfall input as occurs in the Mediterranean climate (Figure 2h). For example, in the Gabilan Mesa sites in California and the Chilean sites, winter precipitation exceeds PET demand (Figures S4 and S5); hence, the vegetation on EFS can benefit from more insolation during this period and grow faster than that on PFS.

Catchments in areas influenced by the NAM have been classified as Type I $NDVI_{diff}$ as PFS have higher NDVI throughout the year. However, these areas may also experience periods in which rainfall exceeds evaporative demand, but only for a short period (much shorter than Mediterranean climate). Results from modeling experiments suggest that energy-limited conditions might occur in the NAM region following intense storms during summer, inducing a short-lived energy-driven advantage for vegetation growth in EFS as compared to the opposite shady PFS areas (Yetemen et al., 2015). However, because of the short-lived and sporadic character of these events, they are unlikely to be captured by the mean monthly values over the entire study period used in our analysis.

Studies from aspect-controlled sites often report the existence of different plant functional types (PFTs) on opposing hillslopes (i.e., tree, shrub, and grass) (Gutiérrez-Jurado et al., 2013). For example, observations from an oak-grass savanna site in California indicate that grasses respond to the onset of the wet season (winter) earlier than trees, which do not respond until spring (Liu et al., 2017). Grasses tend to respond faster to winter rains greening-up before the tree leaf-out period, but trees keep their foliage for a long period after grasses have already senesced (Liu et al., 2017). During winter in the Gabilan Mesa sites, the early greening of grasses on the sunny EFS results in relatively higher NDVI values than PFS which can be covered by oaks. Later, when oaks leaf out in late spring, they can cause the NDVI values on PFS to increase, leading to NDVI values on PFS exceeding those on EFS and seasonal reversal in $NDVI_{diff}$. It is important to note that the relatively faster growth response of grasses on EFS at this site occurs during a period when evapotranspiration is energy limited, which suggests that the phenological difference between PFTs can further promote $NDVI_{diff}$ in favor of EFS for Mediterranean climate when PET demand is exceeded by precipitation input. Chilean sites in the SH, which have similar climate, may follow the same pattern (Figures S4 and S5) (Parsons, 1976).

Though the majority of the sites show seasonal variations in $NDVI_{diff}$, a few sites (~20%) display negligible NDVI differences between opposing hillslopes (Type III pattern). This is the case for the Ramat Avisur (Israel) (Figure 2c) and Erkowit (Sudan) sites. The absence of discernible difference in $NDVI_{diff}$ may be ascribed to the extremely arid climates prevailing at these sites. However, some catchments in the Tabernas Desert (Spain) and Upper Rio Salado (Arizona) also display negligible values of $NDVI_{diff}$, which deviate from the patterns obtained for the other catchments located in the same sites. This might be attributed to regional control of geology and other aspects of stratigraphic dips or bedrock structure and lithology (Churchill, 1981; Richardson et al., 2020; Yetemen et al., 2010).

As explained in section 2, in order to avoid topographic illumination effects, we did not include in our analysis sites with large steepness or ruggedness. Compared to the catchments studied here, steeper catchments may display a more complex topography and a more pronounced aspect-driven effect (Ivanov et al., 2008), which could potentially result in larger NDVI differences. Further research is needed to assess whether transitions from water-limited to energy-limited conditions in steeper and more complex catchments can be effective in producing seasonal reversals in NDVI patterns.

5. Conclusion

Our analyses of climate, topography, and vegetation data from 60 catchments located across all continents, except Antarctica, show that the overwhelming majority of sites display seasonal reversal of vegetation-greenness dominance patterns from PFS to EFS, which can be explained by transitions from water-limited to energy-limited conditions. This research constitutes a first step to better understand variations of vegetation on hillslopes with opposing aspects. Improving the representation of vegetation dynamics in shady and sunny semiarid hillslopes is of great importance to satisfy the growing demand for better ecohydrology models in Earth system (Fan et al., 2019) and landscape evolution frameworks (Yetemen et al., 2019).

Data Availability Statement

Data sets used in this study are publicly available and can be accessed from the following online repositories: Shuttle Radar Topography Mission (SRTM) SRTM 1-arc second global DEM and NDVI from GEE (<https://developers.google.com/earth-engine/datasets>); monthly mean temperature and precipitation from WorldClim (Version2) (worldclim.org); and monthly mean potential evapotranspiration from Consultative Group on International Agricultural Research-Consortium for Spatial Information (CGIAR-CSI) (<https://cgiarcsi.community/data/global-aridity-and-pet-database/>).

Acknowledgments

We thank the editor (Valeriy Y. Ivanov), Todd Hawbaker, and three anonymous reviewers for comments and suggestions which improved the content of this paper. We thank Sandra C. Cooper for thorough and careful technical editing. O. Yetemen acknowledges support from the University of Newcastle Research Advantage for Early Career Researcher (ECR) Higher Degree by Research (HDR) scholarship and the Scientific and Technological Research Council of Turkey (TUBITAK) through Grant 118C329. P. M. Saco acknowledges support from the Australian Research Council through Grants FT140100610 and DP140104178. S. A. Johnstone was supported by the U.S. Geological Survey National Cooperative Geologic Mapping Program. Any use of trade, firm, or product names is for descriptive purposes only and does not imply endorsement by the U.S. Government.

References

- Armesto, J. J., & Martinez, J. A. (1978). Relations between vegetation structure and slope aspect in the Mediterranean region of Chile. *The Journal of Ecology*, *66*(3), 881–889. <https://doi.org/10.2307/2259301>
- Asner, G. P., & Martin, R. E. (2009). Airborne spectranomics: Mapping canopy chemical and taxonomic diversity in tropical forests. *Frontiers in Ecology and the Environment*, *7*(5), 269–276. <https://doi.org/10.1890/070152>
- Badano, E. I., Cavieres, L. A., Molina-Montenegro, M. A., & Quiroz, C. L. (2005). Slope aspect influences plant association patterns in the Mediterranean matorral of central Chile. *Journal of Arid Environments*, *62*(1), 93–108. <https://doi.org/10.1016/j.jaridenv.2004.10.012>
- Barbosa, H. A., Huete, A. R., & Baethgen, W. E. (2006). A 20-year study of NDVI variability over the Northeast Region of Brazil. *Journal of Arid Environments*, *67*(2), 288–307. <https://doi.org/10.1016/j.jaridenv.2006.02.022>
- Becerril-Piña, R., Mastachi-Loza, C. A., González-Sosa, E., Díaz-Delgado, C., & Bã, K. M. (2015). Assessing desertification risk in the semi-arid highlands of central Mexico. *Journal of Arid Environments*, *120*, 4–13. <https://doi.org/10.1016/j.jaridenv.2015.04.006>
- Billingsley, G. H., Priest, S. S., & Felger, T. J. (2008). Geologic map of the Fredonia 30' × 60' quadrangle, Mohave and Coconino counties, northern Arizona (version 1). U.S. Geological Survey Scientific Investigations Map. <https://doi.org/10.3133/sim3035>
- Boisvenue, C., & Running, S. W. (2006). Impacts of climate change on natural forest productivity—Evidence since the middle of the 20th century. *Global Change Biology*, *12*(5), 862–882. <https://doi.org/10.1111/j.1365-2486.2006.01134.x>
- Branson, F. A., & Shown, L. M. (1989). Contrasts of vegetation, soils, microclimates, and geomorphic processes between north- and south-facing slopes on Green Mountain near Denver, Colorado. *U.S. Geological Survey Water Resources Investigation Report*, 89–4094. <https://doi.org/10.3133/wri894094>
- Broza, M., Poliakov, D., Gruia, M., & Bretfeld, G. (2004). Soil collembolan communities on north- and south-facing slopes of an eastern Mediterranean valley. *Pedobiologia*, *48*(5–6), 537–543. <https://doi.org/10.1016/j.pedobi.2004.07.007>
- Calviño-Cancela, M., Chas-Amil, M. L., Garcia-Martínez, E. D., & Touza, J. (2017). Interacting effects of topography, vegetation, human activities and wildland-urban interfaces on wildfire ignition risk. *Forest Ecology and Management*, *397*, 10–17. <https://doi.org/10.1016/j.foreco.2017.04.033>
- Cantón, Y., Solé-Benet, A., & Domingo, F. (2004). Temporal and spatial patterns of soil moisture in semiarid badlands of SE Spain. *Journal of Hydrology*, *285*(1–4), 199–214. <https://doi.org/10.1016/j.jhydrol.2003.08.018>
- Caylor, K. K., Scanlon, T. M., & Rodriguez-Iturbe, I. (2004). Feasible optimality of vegetation patterns in river basins. *Geophysical Research Letters*, *31*, L13502. <https://doi.org/10.1029/2004GL020260>
- Churchill, R. R. (1981). Aspect-related differences in badlands slopes morphology. *Annals of the Association of American Geographers*, *72*(2), 171–182. <https://doi.org/10.1002/esp.3290070209>
- Del Toro-Guerrero, F. J., Hinojosa-Corona, A., & Kretzschmar, T. G. (2016). A comparative study of NDVI values between north- and south-facing slopes in a semiarid mountainous region. *IEEE Journal of Selected Topics in Applied Earth Observations and Remote Sensing*, *9*(12), 5350–5356. <https://doi.org/10.1109/JSTARS.2016.2618393>
- Del-Toro-Guerrero, F. J., Kretzschmar, T., & Bullock, S. H. (2019). Precipitation and topography modulate vegetation greenness in the mountains of Baja California, México. *International Journal of Biometeorology*, *63*(10), 1425–1435. <https://doi.org/10.1007/s00484-019-01763-5>
- Dozier, J. (1989). Spectral signature of alpine snow cover from the Landsat Thematic Mapper. *Remote Sensing of Environment*, *28*, 9–22. [https://doi.org/10.1016/0034-4257\(89\)90101-6](https://doi.org/10.1016/0034-4257(89)90101-6)

- Earles, J. M., Stevens, J. T., Sperling, O., Jessica Orozco, J., North, M. P., & Zwieniecki, M. A. (2018). Extreme mid-winter drought weakens tree hydraulic-carbohydrate systems and slows growth. *New Phytologist*, *219*(1), 89–97. <https://doi.org/10.1111/nph.15136>
- ESRI. (2015). ArcGIS Desktop: Release 10.3.1 Environmental Systems Research Institute, Redlands, CA.
- Fan, Y., Clark, M., Lawrence, D. M., Swenson, S., Band, L. E., Brantley, S. L., et al. (2019). Hillslope hydrology in global change research and earth system modeling. *Water Resources Research*, *55*, 1737–1772. <https://doi.org/10.1029/2018WR023903>
- Farr, T. G., Rosen, P. A., Caro, E., Crippen, R., Duren, R., Hensley, S., et al. (2007). The shuttle radar topography mission. *Reviews of Geophysics*, *45*, RG2004. <https://doi.org/10.1029/2005RG000183>
- Fensholt, R., Sandholt, I., & Rasmussen, M. S. (2004). Evaluation of MODIS LAI, fAPAR and the relation between fAPAR and NDVI in a semi-arid environment using in situ measurements. *Remote Sensing of Environment*, *91*(3–4), 490–507. <https://doi.org/10.1016/j.rse.2004.04.009>
- Fick, S. E., & Hijmans, R. J. (2017). WorldClim 2: New 1-km spatial resolution climate surfaces for global land areas. *International Journal of Climatology*, *37*(12), 4302–4315. <https://doi.org/10.1002/joc.5086>
- Flores-Cervantes, J. H., Istanbuluoglu, E., Vivoni, E. R., Holfield Collins, C. D., & Bras, R. L. (2014). A geomorphic perspective on terrain-modulated organization of vegetation productivity: Analysis in two semiarid grassland ecosystems in southwestern United States. *Ecohydrology*, *7*(2), 242–257. <https://doi.org/10.1002/eco.1333>
- García, M., Fernández, N., Villagarcía, L., Domingo, F., Puigdefàbregas, J., & Sandholt, I. (2014). Accuracy of the Temperature-Vegetation Dryness Index using MODIS under water-limited vs. energy-limited evapotranspiration conditions. *Remote Sensing of Environment*, *149*, 100–117. <https://doi.org/10.1016/j.rse.2014.04.002>
- Geoy, I. J., Gribb, M. M., Marshall, H. P., Chandler, D. G., Benner, S. G., & Mcnamara, J. P. (2011). Aspect influences on soil water retention and storage. *Hydrological Processes*, *25*(25), 3836–3842. <https://doi.org/10.1002/hyp.8281>
- Gorelick, N., Hancher, M., Dixon, M., Ilyushchenko, S., Thau, D., & Moore, R. (2017). Google Earth Engine: Planetary-scale geospatial analysis for everyone. *Remote Sensing of Environment*, *202*, 18–27. <https://doi.org/10.1016/j.rse.2017.06.031>
- Gutiérrez-Jurado, H. A., Vivoni, E. R., Cikoski, C., Harrison, B. J., Bras, R. L., & Istanbuluoglu, E. (2013). On the observed ecohydrologic dynamics of a semiarid basin with aspect-delimited ecosystems. *Water Resources Research*, *49*, 8263–8284. <https://doi.org/10.1002/2013WR014364>
- Gutiérrez-Jurado, H. A., Vivoni, E. R., Harrison, J. B. J., & Guan, H. (2006). Ecohydrology of root zone water fluxes and soil development in complex semiarid rangelands. *Hydrological Processes*, *20*(15), 3289–3316. <https://doi.org/10.1002/hyp.6333>
- Hinckley, E. L. S., Ebel, B. A., Barnes, R. T., Anderson, R. S., Williams, M. W., & Anderson, S. P. (2014). Aspect control of water movement on hillslopes near the rain-snow transition of the Colorado Front Range. *Hydrological Processes*, *28*(1), 74–85. <https://doi.org/10.1002/hyp.9549>
- Hoek van Dijke, A. J., Mallick, K., Teuling, A. J., Schlerf, M., Machwitz, M., Hassler, S. K., et al. (2019). Does the Normalized Difference Vegetation Index explain spatial and temporal variability in sap velocity in temperate forest ecosystems? *Hydrology and Earth System Sciences*, *23*(4), 2077–2091. <https://doi.org/10.5194/hess-23-2077-2019>
- Holben, B. N., & Justice, C. O. (1980). The topographic effect on spectral response from nadir-pointing sensors. *Photogrammetric Engineering and Remote Sensing*, *46*(9), 1191–1200.
- Huete, A., Didan, K., Miura, T., Rodriguez, E. P., Gao, X., & Ferreira, L. G. (2002). Overview of the radiometric and biophysical performance of the MODIS vegetation indices. *Remote Sensing of Environment*, *83*(1–2), 195–213. [https://doi.org/10.1016/S0034-4257\(02\)00096-2](https://doi.org/10.1016/S0034-4257(02)00096-2)
- Ivanov, V. Y., Bras, R. L., & Vivoni, E. R. (2008). Vegetation-hydrology dynamics in complex terrain of semiarid areas: 2. Energy-water controls of vegetation spatiotemporal dynamics and topographic niches of favorability. *Water Resources Research*, *44*, W03430. <https://doi.org/10.1029/2006WR005595>
- Jin, X., Wan, L., Zhang, Y. K., Hu, G., Schaepman, M. E., Clevers, J. G. P. W., & Su, Z. B. (2009). Quantification of spatial distribution of vegetation in the Qilian Mountain area with MODIS NDVI. *International Journal of Remote Sensing*, *30*(21), 5751–5766. <https://doi.org/10.1080/01431160902736635>
- Johnstone, S. A., Finnegan, N. J., & Hilley, G. E. (2017). Weak bedrock allows north-south elongation of channels in semi-arid landscapes. *Earth and Planetary Science Letters*, *478*, 150–158. <https://doi.org/10.1016/j.epsl.2017.08.037>
- Justice, C. O., Wharton, S. W., & Holben, B. N. (1981). Application of digital terrain data to quantify and reduce the topographic effect on Landsat data. *International Journal of Remote Sensing*, *2*(3), 213–230. <https://doi.org/10.1080/01431168108948358>
- Kirkpatrick, J. B., & Nunez, M. (1980). Vegetation-radiation relationships in mountainous terrain: Eucalypt-dominated vegetation in the Risdon Hills, Tasmania. *Journal of Biogeography*, *7*(2), 197. <https://doi.org/10.2307/2844711>
- Klein, A. G., Hall, D. K., & Riggs, G. A. (1998). Improving snow cover mapping in forests through the use of a canopy reflectance model. *Hydrological Processes*, *12*(10–11), 1723–1744. [https://doi.org/10.1002/\(SICI\)1099-1085\(199808/09\)12:10<1723::AID-HYP691>3.0.CO;2-2](https://doi.org/10.1002/(SICI)1099-1085(199808/09)12:10<1723::AID-HYP691>3.0.CO;2-2)
- Klemmedson, J. O., & Wienhold, B. J. (1992). Aspect and species influences on nitrogen and phosphorus accumulation in Arizona chaparral soil-plant systems. *Arid Soil Research and Rehabilitation*, *6*(2), 105–116. <https://doi.org/10.1080/15324989209381303>
- Kunkel, M. L., Flores, A. N., Smith, T. J., McNamara, J. P., & Benner, S. G. (2011). A simplified approach for estimating soil carbon and nitrogen stocks in semi-arid complex terrain. *Geoderma*, *165*(1), 1–11. <https://doi.org/10.1016/j.geoderma.2011.06.011>
- Lawley, V., Lewis, M., Clarke, K., & Ostendorf, B. (2016). Site-based and remote sensing methods for monitoring indicators of vegetation condition: An Australian review. *Ecological Indicators*, *60*, 1273–1283. <https://doi.org/10.1016/j.ecolind.2015.03.021>
- Liu, G., Liu, H., & Yin, Y. (2013). Global patterns of NDVI-indicated vegetation extremes and their sensitivity to climate extremes. *Environmental Research Letters*, *8*(2), 025009. <https://doi.org/10.1088/1748-9326/8/2/025009>
- Liu, Y., Hill, M. J., Zhang, X., Wang, Z., Richardson, A. D., Hufkens, K., et al. (2017). Using data from Landsat, MODIS, VIIRS and PhenoCams to monitor the phenology of California oak/grass savanna and open grassland across spatial scales. *Agricultural and Forest Meteorology*, *237–238*, 311–325. <https://doi.org/10.1016/j.agrformet.2017.02.026>
- Martín-Ortega, P., García-Montero, L. G., & Sibelet, N. (2020). Temporal patterns in illumination conditions and its effect on vegetation indices using Landsat on Google Earth Engine. *Remote Sensing*, *12*(2), 211. <https://doi.org/10.3390/rs12020211>
- Matsushita, B., Yang, W., Chen, J., Onda, Y., & Qiu, G. (2007). Sensitivity of the Enhanced Vegetation Index (EVI) and Normalized Difference Vegetation Index (NDVI) to topographic effects: A case study in high-density cypress forest. *Sensors*, *7*(11), 2636–2651. <https://doi.org/10.3390/s7112636>
- McGuire, L. A., Pelletier, J. D., & Roering, J. J. (2014). Development of topographic asymmetry: Insights from dated cinder cones in the western United States. *Journal of Geophysical Research: Earth Surface*, *119*, 1725–1750. <https://doi.org/10.1002/2014JF003081>

- Metzen, D., Sheridan, G. J., Benyon, R. G., Bolstad, P. V., Griebel, A., & Lane, P. N. J. (2019). Spatio-temporal transpiration patterns reflect vegetation structure in complex upland terrain. *Science of the Total Environment*, 694, 133551. <https://doi.org/10.1016/j.scitotenv.2019.07.357>
- Moran, M. S., Scott, R. L., Keefer, T. O., Emmerich, W. E., Hernandez, M., Nearing, G. S., et al. (2009). Partitioning evapotranspiration in semiarid grassland and shrubland ecosystems using time series of soil surface temperature. *Agricultural and Forest Meteorology*, 149(1), 59–72. <https://doi.org/10.1016/j.agrformet.2008.07.004>
- Moreira, E. P., & Valeriano, M. M. (2014). Application and evaluation of topographic correction methods to improve land cover mapping using object-based classification. *International Journal of Applied Earth Observation and Geoinformation*, 32, 208–217. <https://doi.org/10.1016/j.jag.2014.04.006>
- Moreno-De Las Heras, M., Saco, P. M., Willgoose, G. R., & Tongway, D. J. (2012). Variations in hydrological connectivity of Australian semiarid landscapes indicate abrupt changes in rainfall-use efficiency of vegetation. *Journal of Geophysical Research*, 117, G03009. <https://doi.org/10.1029/2011JG001839>
- Nagendra, H. (2001). Using remote sensing to assess biodiversity. *International Journal of Remote Sensing*, 22(12), 2377–2400. <https://doi.org/10.1080/01431160117096>
- Nevo, E. (1995). Asian, African and European biota meet at “Evolution Canyon” Israel: Local tests of global biodiversity and genetic diversity patterns. *Proceedings of the Royal Society B: Biological Sciences*, 262(1364), 149–155. <https://doi.org/10.1098/rspb.1995.0189>
- Nobel, P. S., & Linton, M. J. (1997). Frequencies, microclimate and root properties for three codominant perennials in the northwestern Sonoran Desert on north- vs. south-facing slopes. *Annals of Botany*, 80(6), 731–739. <https://doi.org/10.1006/anbo.1997.0508>
- Parsons, D. J. (1976). Vegetation structure in the Mediterranean scrub communities of California and Chile. *The Journal of Ecology*, 64(2), 435. <https://doi.org/10.2307/2258767>
- Pelletier, J. D., & Swetnam, T. L. (2017). Asymmetry of weathering-limited hillslopes: The importance of diurnal covariation in solar insolation and temperature. *Earth Surface Processes and Landforms*, 42(9), 1408–1418. <https://doi.org/10.1002/esp.4136>
- Pettorelli, N., Vik, J. O., Mysterud, A., Gaillard, J. M., Tucker, C. J., & Stenseth, N. C. (2005). Using the satellite-derived NDVI to assess ecological responses to environmental change. *Trends in Ecology & Evolution*, 20(9), 503–510. <https://doi.org/10.1016/j.tree.2005.05.011>
- Richardson, P. W., Perron, J. T., Miller, S. R., & Kirchner, J. W. (2020). Unraveling the mysteries of asymmetric topography at Gabilan Mesa, California. *Journal of Geophysical Research: Earth Surface*, 125, e2019JF005378. <https://doi.org/10.1029/2019JF005378>
- Riggs, G. A., Hall, D. K., & Román, M. O. (2017). Overview of NASA’s MODIS and Visible Infrared Imaging Radiometer Suite (VIIRS) snow-cover Earth System Data Records. *Earth System Science Data*, 9(2), 765–777. <https://doi.org/10.5194/essd-9-765-2017>
- Rittger, K., Painter, T. H., & Dozier, J. (2013). Assessment of methods for mapping snow cover from MODIS. *Advances in Water Resources*, 51, 367–380. <https://doi.org/10.1016/j.advwatres.2012.03.002>
- Román-Sánchez, A., Vanwallegem, T., Peña, A., Laguna, A., & Giráldez, J. V. (2018). Controls on soil carbon storage from topography and vegetation in a rocky, semi-arid landscapes. *Geoderma*, 311, 159–166. <https://doi.org/10.1016/j.geoderma.2016.10.013>
- Rouse, J. W., Haas, R. H., Schell, J. A., & Deering, D. W. (1973). Monitoring the vernal advancement and retrogradation (green wave effect) of natural vegetation. Progress Report RSC 1978–1971.
- Salzer, M. W., Larson, E. R., Bunn, A. G., & Hughes, M. K. (2014). Changing climate response in near-treeline bristlecone pine with elevation and aspect. *Environmental Research Letters*, 9(11), 114007. <https://doi.org/10.1088/1748-9326/9/11/114007>
- Shabanov, N. V., Zhou, L., Knyazikhin, Y., Myneni, R. B., & Tucker, C. J. (2002). Analysis of interannual changes in northern vegetation activity observed in AVHRR data from 1981 to 1994. *IEEE Transactions on Geoscience and Remote Sensing*, 40(1), 115–130. <https://doi.org/10.1109/36.981354>
- Sternberg, M., & Shoshany, M. (2001). Influence of slope aspect on Mediterranean woody formations: Comparison of a semiarid and an arid site in Israel. *Ecological Research*, 16(2), 335–345. <https://doi.org/10.1046/j.1440-1703.2001.00393.x>
- Teillet, P. M., Guindon, B., & Goodenough, D. G. (1982). On the slope-aspect correction of multispectral scanner data. *Canadian Journal of Remote Sensing*, 43(9), 2148–2159. <https://doi.org/10.1109/TGRS.2005.852480>
- Vetaas, O. R. (1992). Gradients in field-layer vegetation on an arid misty mountain plateau in the Sudan. *Journal of Vegetation Science*, 3(4), 527–534. <https://doi.org/10.2307/3235809>
- Wallace, J., Behn, G., & Furby, S. (2006). Vegetation condition assessment and monitoring from sequences of satellite imagery. *Ecological Management and Restoration*, 7(SUPPL. 1), S31–S36. <https://doi.org/10.1111/j.1442-8903.2006.00289.x>
- Walsh, S. F., Nyman, P., Sheridan, G. J., Baillie, C. C., Tolhurst, K. G., & Duff, T. J. (2017). Hillslope-scale prediction of terrain and forest canopy effects on temperature and near-surface soil moisture deficit. *International Journal of Wildland Fire*, 26(3), 191–208. <https://doi.org/10.1071/WF16106>
- Xu, X., Guan, H., Skrzypek, G., & Simmons, C. T. (2017). Response of leaf stable carbon isotope composition to temporal and spatial variabilities of aridity index on two opposite hillslopes in a native vegetated catchment. *Journal of Hydrology*, 553, 214–223. <https://doi.org/10.1016/j.jhydrol.2017.05.062>
- Yetemen, O., Istanbuluoglu, E., Flores-Cervantes, J. H., Vivoni, E. R., & Bras, R. L. (2015). Ecohydrologic role of solar radiation on landscape evolution. *Water Resources Research*, 51, 1127–1157. <https://doi.org/10.1002/2014WR016169>
- Yetemen, O., Istanbuluoglu, E., & Vivoni, E. R. (2010). The implications of geology, soils, and vegetation on landscape morphology: Inferences from semi-arid basins with complex vegetation patterns in Central New Mexico, USA. *Geomorphology*, 116(3–4), 246–263. <https://doi.org/10.1016/j.geomorph.2009.11.026>
- Yetemen, O., Saco, P. M., & Istanbuluoglu, E. (2019). Ecohydrology controls the geomorphic response to climate change. *Geophysical Research Letters*, 46, 8852–8861. <https://doi.org/10.1029/2019GL083874>
- Zhang, W., Jiang, Y., Wang, M., Zhang, L., & Dong, M. (2015). Topography- and species-dependent climatic responses in radial growth of *Picea meyeri* and *Larix principis-rupprechtii* in the Luyashan Mountains of North-Central China. *Forests*, 6(12), 116–132. <https://doi.org/10.3390/f6010116>
- Zomer, R. J., Trabucco, A., Bossio, D. A., & Verchot, L. V. (2008). Climate change mitigation: A spatial analysis of global land suitability for clean development mechanism afforestation and reforestation. *Agriculture, Ecosystems and Environment*, 126(1–2), 67–80. <https://doi.org/10.1016/j.agee.2008.01.014>
- Zou, C. B., Barron-Gafford, G. A., & Breshears, D. D. (2007). Effects of topography and woody plant canopy cover on near-ground solar radiation: Relevant energy inputs for ecohydrology and hydrogeology. *Geophysical Research Letters*, 34, L24S21. <https://doi.org/10.1029/2007GL031484>

Reference From the Supporting Information

Soenen, S. A., Peddle, D. R., & Coburn, C. A. (2005). SCS+ C: A modified sun-canopy-sensor topographic correction in forested terrain. *IEEE Transactions on Geoscience and Remote Sensing*, 43(9), 2148–2159. <https://doi.org/10.1109/TGRS.2005.852480>